



Available online at <http://scik.org>

J. Math. Comput. Sci. 3 (2013), No. 5, 1252-1270

ISSN: 1927-5307

## EXTRACT RIDGES AND RAVINES USING HESSIAN MATRIX OF 3D IMAGE

NASSAR H. ABDEL-ALL, M. A. SOLIMAN, R. A. HUSSIEN, AND WADAH M. EL-NINI\*

Department of Mathematics, Faculty of Science, Assiut University, Assiut, Egypt

**Abstract.** Edge detection in two and three-dimensional images is used to located points corresponding to surfaces of three dimension (3D) structures. The next stage is to characterize the local geometry of these surfaces in order to extract points or lines which may be used by registration and tracking procedures. Typically one must calculate second-order differential characteristics of the surfaces such as the maximum, mean, and Gaussian curvatures. Assuming that the surface is defined locally by a isointensity contour. One can calculate directly the curvatures and characterize the local curvature extrema (ridge points) from the first, second, and third derivatives of the vector valued function. These partial derivatives are computed using the operators of the edge detection.

**Keywords:** Hessian Matrix; Ridges and Ravines.

**2010 AMS Subject Classification:** 15A18; 53A05

### 1. Introduction

Edge detection in 2D and 3D images is used to located points corresponding to surfaces of 3D structures [19, 20, 33]. The next stage is to characterize the local geometry of these surfaces in order to extract points or lines which may be used by registration, tracking, and matching procedures [6, 15, 25, 28]. Typically one must calculate second-order differential

---

\*Corresponding author

Received Jul 19, 2013

characteristics of the surfaces such as the maximum, mean, and Gaussian curvatures. The classical scheme is to use local surface fitting on the adjacency graph defined by the edge points [27]. One faces the problem of linking surface elements detected by 3D edge operators and local surface approximation, which may be done taking uncertainty into account [18].

In this paper we show how to compute the curvature of the surface defined by the equation (or the edge points) from the second partial derivatives of the image. The partial derivatives of the 3-dimension image can be computed using the same operators as those used for edge detection [19]. We will propose two methods.

By assuming that the surface is defined by an isocontour (i.e., the 3D gradient at an edge point corresponds to the normal to the surface), one can compute directly the curvatures and characterize the local curvature extrema (ridge points will be discussed in more detail in Section (3)) from the first, second, and third derivative of the vector valued function.

The paper is organized as follows. In the second section we reviews concepts from differential geometry utilized in this paper. In the third section we reviews concepts from ridge and ravine. The fourth section deals with the direct computation of the curvatures using the gradient and Hessian matrix (i.e. the first and second partial derivatives of isosurface). In the fifth section deals with the direct computation of the ridge points using the gradient, Hessian matrix and its derivatives (i.e. the first, second, third and fourth partial derivatives) of isosurface. In the sixth section presents a practical algorithm based on the previous development. In the seventh section gives experimental results in the two- and three-dimensional images.

## 2. Differential geometry of surfaces

This section reviews concepts from differential geometry utilized in this paper. We provide intuitive descriptions and refer the reader to O'Neill for formality [24].

The term "surface" is often loosely used in the literature. The definitions in this paper assume the surface to be **isosurface** in  $R^3$ , i.e., the 3D gradient at a contour point (an

edge point on 3D image) corresponds to the normal to the surface. Figure 1 shows surface  $M$  and the neighborhood around a point  $p$  on the surface.

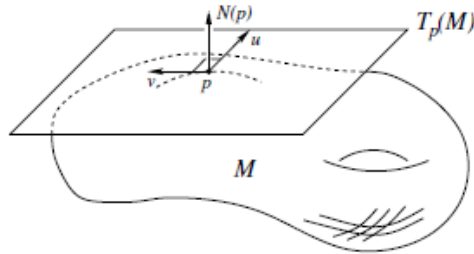


FIGURE 1. Surface  $M$  with tangent plane  $T_p(M)$  at point  $p$ . The coordinate frame  $(u, v)$  at  $p$  locally parameterizes  $T_p(M)$ .

Let  $p \in M$  be a point on the surface  $M$ . One can intuitively understand what it means for a vector to be **tangent** to a surface  $M$ . The formal definition is based on the idea that a vector tangent to  $M$  at  $p$  must be a tangent vector of a curve lying in  $M$  passing through  $p$ . The set of all tangent vectors to  $M$  at  $p$  is the **tangent plane**  $T_p(M)$ , the best linear approximation of the surface at  $p$ , as shown in Figure 1. The vector  $N(p)$  is **normal** to  $M$  at  $p$ , i.e., it is orthogonal to the tangent plane  $T_p(M)$  and therefore to every tangent vector to  $M$  at  $p$ .

To study how  $M$  bends at point  $p$  in tangent direction  $v$ , we intersect  $M$  with a plane containing both  $v$  and  $N(p)$ . This "normal section" of  $M$  is a curve in  $M$ , as indicated in Figure 2.

The **curvature** of this curve at  $p$  is called the **normal curvature** of  $M$  at  $p$  in the  $v$  direction and is denoted by  $\kappa(v)$ . where  $v$  is a unit tangent vector.

Let us fix  $p$  and imagine that the unit tangent vector  $v$  at  $p$  revolves about  $N(p)$  in the tangent plane  $T_p(M)$ . The normal section corresponding to the different tangent directions give us a moving picture of the way  $M$  is bending in every tangent direction at  $p$ . Using this scheme, it is easy to pick out the directions of maximum and minimum bending. The maximum and minimum values of normal curvature  $\kappa$  over all possible tangent directions at  $p$  are called the **principal curvatures** of  $M$  at  $p$ , denoted  $\kappa_1$  and  $\kappa_2$  respectively. The directions in which these extreme values occur are called the **principal directions** of  $M$

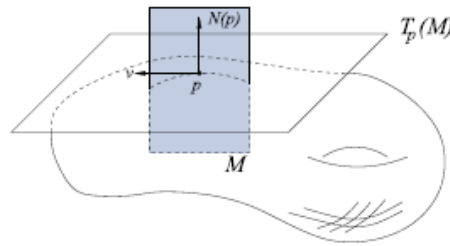


FIGURE 2. Normal section (dotted curve) of surface  $M$  at point  $p$  in tangent direction  $v$ , obtained by intersection of  $M$  with plane (shaded) containing  $v$  and  $N(p)$ .

at  $p$ . The unit vectors in these directions are called the **principal vectors** of  $M$  at  $p$ , denoted  $t_1$  and  $t_2$ , respectively.

The **Gaussian** curvature  $\kappa_g$  of  $M$  at  $p$  is defined as the product of the principal curvatures,

$$\kappa_g = \kappa_1 \kappa_2. \quad (2.1)$$

The **mean** curvature  $\kappa_m$  of  $M$  at  $p$  is defined as the average of the principal curvatures,

$$\kappa_m = \frac{\kappa_1 + \kappa_2}{2}. \quad (2.2)$$

### 3. Ridges and Ravines

Surface creases provide us with important information about the shapes of objects and can be intuitively defined as curves on a surface along which the surface bends sharply. mathematical description of surface creases is based on study of extrema of the principal curvatures along their curvature lines. Besides the mathematical beauty of such surface features [26], they have been studied in connection with applications in image and data analysis [12, 31], face recognition [13], quality control of free-form surfaces [14], analysis of medical images [5, 8, 18, 29] and satellite data [21]. See also references therein. Shape description with curvature extrema has been a subject of research in [16, 17].

Assume that the maximal and minimal curvatures  $k_{max} = \kappa_1$  and  $k_{min} = \kappa_2$  of  $M$  at  $p$ . The associated tangent directions  $t_{max} = t_1$  and  $t_{min} = t_2$  of  $M$  at  $p$ . The integral curves

of the principal direction fields are called the **curvature lines**. A point at which one of the principal curvatures vanishes is called **parabolic**. A point at which the principal curvatures are equal to each other is called **umbilic**. The principal centers of curvature are the points situated on the surface normal passing through  $p$  at distances  $\kappa_{max}^{-1}$  and  $\kappa_{min}^{-1}$  from  $p$ . The loci of the principal centers form the caustic. The caustic consists of two sheets corresponding to the maximal and minimal principal curvatures [2, 3, 4].

**Definition 3.1.** *A non-umbilic point  $p \in M$  is called a **ridge point** if  $\kappa_{max}$  attains a local positive maximum at  $p$  along the associated curvature line. A non-umbilic point  $q \in M$  is called a **ravine point** if  $\kappa_{min}$  attains a local negative minimum at  $q$  along the associated curvature line.*

**Remark 3.1.** *Although in this definition we deal with nonumbilic points the umbilics can be treated by continuity.*

**Remark 3.2.** *The definitions of the ridges and ravines are dual: if we change the surface orientation then the ridges turn into the ravines and vice versa. Without loss of generality we can consider only the ridges.*

**Remark 3.3.** *In the mathematical part of our research we deal with generic phenomena. Roughly speaking, a particular property of an object from a particular class of objects is generic if in the space of all the objects of that class the objects exhibiting the property form an open dense set.*

## 4. Curvatures from partial derivative

In this section, we give the formulas for computing curvatures using only the information from partial derivatives of the image.

### 4.1. 2D Image

We first present the case in 2D in order to motivate the computations in 3D.

Let  $C$  be an isocontour on an image  $I = I(x, y)$  ( $I$  is differentiable function). the gradient  $\nabla I = (I_x, I_y)^T = \mathbf{g}$  of  $I$  which will lie along the normal of the curve  $C$ , as shown in Figure 3.

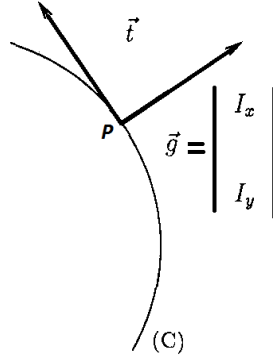


FIGURE 3. 2D isocontour.

We compute the curvature  $\kappa$  of  $C$  at point  $p$ . Let  $\mathbf{t}$  be the curve unit tangent vector to  $C$  at point  $p$ :

$$\mathbf{g} \cdot \mathbf{t} = 0 \quad (4.1)$$

Letting  $s$  be the arclength parameter, we have

$$\frac{d(\mathbf{g} \cdot \mathbf{t})}{ds} = \frac{d\mathbf{g}}{ds} \cdot \mathbf{t} + \mathbf{g} \cdot \frac{d\mathbf{t}}{ds} = 0. \quad (4.2)$$

The curvature  $\kappa$  is obtained by

$$\frac{d\mathbf{t}}{ds} = \kappa \mathbf{n} = \kappa \frac{\mathbf{g}}{\|\mathbf{g}\|}, \quad (4.3)$$

where  $\mathbf{n}$  is the curve unit normal vector (equal to  $\frac{\mathbf{g}}{\|\mathbf{g}\|}$ ). We must suppose here that the normal vector field is regular over the whole image to apply the chain rule. That is an approximation because the contour is not defined everywhere. We also identify the normal vector field to the gradient vector field, which is correct in the case of isocontours. This field is regular because it is issued from a filtering technique. We note that this interpretation problem does not arise in the local contour fitting algorithm where only

the contour points are taken into account. Further assuming that  $\mathbf{g}$  is defined everywhere and is a  $C^2$  mapping from  $\mathbf{R}$  to  $\mathbf{R}^2$ , the chain rule gives

$$\frac{d\mathbf{g}}{ds} = \frac{\partial \mathbf{g}}{\partial x} \frac{dx}{ds} + \frac{\partial \mathbf{g}}{\partial y} \frac{dy}{ds} = \mathbf{H}\mathbf{t}, \tag{4.4}$$

where  $\mathbf{g}$  is the gradient vector and  $\mathbf{H}$  is the Hessian of the gray level function  $I(x, y)$ :

$$\mathbf{g} = \begin{pmatrix} I_x \\ I_y \end{pmatrix}, \quad \mathbf{H} = \begin{pmatrix} I_{xx} & I_{xy} \\ I_{xy} & I_{yy} \end{pmatrix}. \tag{4.5}$$

By combining Eqs.(4.2)-(4.4) we obtain

$$\kappa = \frac{-\mathbf{t}^T \mathbf{H} \mathbf{t}}{\|\mathbf{g}\|}. \tag{4.6}$$

The tangent  $\mathbf{t}$  can be computed simply as

$$\mathbf{t} = \begin{pmatrix} -I_y \\ I_x \end{pmatrix} / \|\mathbf{g}\|. \tag{4.7}$$

### 4.2. 3D Image

We consider a surface  $\mathbf{M}$  defined as an isosurface of  $I(x, y, z)$ . Let  $\mathbf{t}$  be any unit vector in the tangent plane  $T_p$  at a point  $p$  and  $\mathbf{g}$  the normal to  $\mathbf{M}$  at  $p$  as shown in Figure 1. we compute the curvature of  $\mathbf{M}$  in direction  $\mathbf{t}$  which we denote by  $\kappa_t$ .

Using Eq.(4.1), and taking a directional derivative in the direction  $\mathbf{t}$ , we obtain as in the 2D case

$$L_t(\mathbf{g} \cdot \mathbf{t}) = \mathbf{t}^T \mathbf{H} \mathbf{t} + \kappa_t \mathbf{g} \cdot \mathbf{n} = 0,$$

where  $L_t$  is the Lie derivation operator and  $\mathbf{H}$  is the Hessian of the gray level function  $I(x, y, z)$  [23]:

$$\mathbf{H} = \begin{pmatrix} I_{xx} & I_{xy} & I_{xz} \\ I_{xy} & I_{yy} & I_{yz} \\ I_{xz} & I_{yz} & I_{zz} \end{pmatrix}, \quad \mathbf{g} = \begin{pmatrix} I_x \\ I_y \\ I_z \end{pmatrix}. \quad (4.8)$$

Since  $\mathbf{n} = \frac{\mathbf{g}}{\|\mathbf{g}\|}$  and using

$$\frac{d\mathbf{g}}{ds} = \mathbf{H}\mathbf{t}, \quad (4.9)$$

and

$$\frac{d\mathbf{t}}{ds} = \kappa_t \mathbf{n} = \kappa_t \frac{\mathbf{g}}{\|\mathbf{g}\|}, \quad (4.10)$$

we obtain

$$\kappa_t = \frac{-t^T H t}{\|g\|}. \quad (4.11)$$

The principal curvatures and the principal directions can be computed by searching the directions  $\mathbf{t}$  for which  $\kappa_t$  is an extremum using the vector calculus. Let  $\mathbf{a}$  and  $\mathbf{b}$  form an orthonormal basis of tangent plane to the surface, thus

$$\mathbf{t} = \cos \theta \mathbf{a} + \sin \theta \mathbf{b}.$$

If we derive  $\kappa_t$  with respect to  $\theta$ , we obtain

$$-\|\mathbf{g}\| \frac{d\kappa_t}{d\theta} = \frac{d(t^T H t)}{d\theta} = (b^T H b - a^T H a) \sin 2\theta + 2a^T H b \cos 2\theta.$$

Then if  $\theta$  is a principal direction this derivative is equal to 0, i.e.,

$$\frac{\partial \kappa_t}{\partial \theta} = 0 \Leftrightarrow \tan 2\theta = \frac{2a^T H b}{a^T H a - b^T H b} = E \Leftrightarrow \left( \theta = \theta_1 = \frac{\arctan E}{2} \right) \vee \left( \theta = \theta_2 = \theta_1 + \frac{\pi}{2} \right)$$

we note that the first equivalence requires that the denominator does not vanish. In fact, the denominator is zero if and only if the point is an umbilic point (see section 3). The two principal directions  $\mathbf{t}_1$  and  $\mathbf{t}_2$  are

$$\mathbf{t}_1 = \cos \theta_1 \mathbf{a} + \sin \theta_1 \mathbf{b}, \quad \mathbf{t}_2 = \cos \theta_2 \mathbf{a} + \sin \theta_2 \mathbf{b}. \quad (4.12)$$



The two principal curvatures are

$$\kappa_{t_1} = -\frac{t_1^T H t_1}{\|g\|}, \quad \kappa_{t_2} = -\frac{t_2^T H t_2}{\|g\|} \tag{4.13}$$

Henceforth we will assume that  $|\kappa_{t_1}| > |\kappa_{t_2}|$ , i.e.,  $\mathbf{t}_1$  is the maximum curvature direction and  $\kappa_{t_1}$  the maximum curvature.

In order to avoid the arctangent computation, we use the following method to find the principal curvatures and the principal directions.

The principal curvatures may be characterized as the solution to the constrained optimization problem:

$$\begin{aligned} & \text{Min } \langle Ht, t \rangle \\ & \text{s.c. } \begin{cases} \langle t, t \rangle = 1 \\ \langle t, g \rangle = 0. \end{cases} \end{aligned} \tag{4.14}$$

We define a rotation matrix  $P$  to change coordinates so that the first basis vector is rotated to the direction  $\mathbf{g}$ ,

$$\mathbf{P} = \begin{pmatrix} I_x/\delta & I_y/\gamma & I_z I_x/\delta\gamma \\ I_y/\delta & -I_x/\gamma & I_y I_z/\delta\gamma \\ I_z/\delta & 0 & -\gamma/\delta \end{pmatrix} = \begin{pmatrix} n & h & f \end{pmatrix}. \tag{4.15}$$

with  $\gamma = \sqrt{I_x^2 + I_y^2}$ ,  $\delta = \sqrt{I_x^2 + I_y^2 + I_z^2} = \|g\|$  and  $n = g/\delta$ .

After using the linear transformation,  $Pw = t$  the minimization problem (4.14) becomes

$$\begin{aligned} & \text{Min } \langle HPw, Pw \rangle \\ & \text{s.c. } \begin{cases} \langle w, w \rangle = 1 \\ w_1 = 0, \quad \text{with } w = (w_1, w_2, w_3)^T. \end{cases} \end{aligned} \tag{4.16}$$

Introducing the notations

$$\mathbf{H}' = P^T H P = \begin{pmatrix} \cdot & \cdot & \cdot \\ \cdot & & H'_e \\ \cdot & & \cdot \end{pmatrix}, \quad w = \begin{pmatrix} \cdot \\ \cdot \\ w_e \end{pmatrix}, \quad (4.17)$$

we obtain the equivalent problem

$$\begin{aligned} \text{Min } & \langle H'_e w_e, w_e \rangle \\ \text{s.c. } & \langle w_e, w_e \rangle = 1. \end{aligned} \quad (4.18)$$

Using the Lagrange multipliers technique, the problem (4.18) can be reduced to the diagonalization of the matrix  $H'_e$ . The eigenvalues of matrix  $H'_e$  correspond to the principal curvatures. The principal curvature directions are obtained by applying the matrix  $P$  to the eigenvectors of  $H'_e$ . This scheme makes it possible to express principal curvatures  $\kappa_i$  and principal directions  $\mathbf{t}_i$  using only first and second derivatives of the images:

$$\kappa_i = \frac{h^T H h + f^T H f \pm \sqrt{(h^T H h + f^T H f)^2 + 4((h^T H f)^2 - (h^T H h)(f^T H f))}}{2\|g\|} \quad (4.19)$$

The eigenvectors of  $H'_e$  are

$$\mathbf{v}_i = \begin{pmatrix} \lambda_i \\ \cdot \\ 1 \end{pmatrix}, \quad \text{with } \lambda_i = (\kappa_i \|g\| - f^T H f) / f^T H h, \quad i = 1, 2. \quad (4.20)$$

by applying the matrix  $P$  to  $\mathbf{v}_i$ , we obtain

$$\mathbf{t}_i = f + \lambda_i h, \quad \text{with } i = 1, 2. \quad (4.21)$$

**Remark 4.1.** *If  $\kappa_1 \neq \kappa_2$ , then, principal directions  $t_1, t_2$  corresponding to  $\kappa_1, \kappa_2$  respectively are perpendicular.*

*Proof:*  $\langle t_1, t_2 \rangle = 1 + \lambda_1 \lambda_2 = 0$ .

### 5. Characterizing ridge points from the partial derivatives

Ridge from the partial derivatives of the two principal curvature at a point, one has the maximum curvature. The associated direction is the maximum curvature direction. We will call a ridge point any point whose curvature in the maximum curvature direction is locally maximal, and a valley (ravine) point a point where the curvature is minimum in the maximum curvature direction. That is, the maximum curvature value along integrals of the maximum curvature vector field has a local extremum at a ridge or valley point.

#### 5.1. 2D Image

It is of interest to study first the 2D case which presents no ambiguity (see Figure 3).

The 2D contour can be represented by a curve  $(x(s), y(s))$ , where  $s$  the arclength parameter. The curvature  $\kappa(s)$  is given by Eq.(4.6) as:

$$\kappa(s) = \frac{-t^T H t}{\|g\|}, \quad \text{with } \|g\|t = \begin{pmatrix} -I_y \\ I_x \end{pmatrix}, \quad \text{and } t = \begin{pmatrix} x'(s) \\ y'(s) \end{pmatrix}.$$

The curvature extrema are located where the derivative  $\kappa'(s)$  is zero, i.e.,

$$\frac{(d(t^T H t)/ds)\|g\| - (t^T H t)(d\|g\|/ds)}{\|g\|^2} = 0.$$

From Eq.(4.4), one can obtain the following formula

$$\frac{d\|g\|}{ds} = \frac{g^T H t}{\|g\|}.$$

Routine calculation, we have

$$\begin{aligned} \frac{d(t^T H t)}{ds} &= \frac{dt^T}{ds} H t + t^T \frac{d(H t)}{ds} \\ \frac{d(H t)}{ds} &= \begin{pmatrix} t^T H_x t \\ t^T H_y t \end{pmatrix} + H \frac{dt}{ds} \end{aligned}$$

$$\text{with } H_x = \begin{pmatrix} I_{xxx} & I_{xyx} \\ I_{yxx} & I_{yyx} \end{pmatrix}, \quad H_y = \begin{pmatrix} I_{xxy} & I_{xyy} \\ I_{yxx} & I_{yyx} \end{pmatrix}.$$

Thus, the curvature extrema are finally defined by the formula

$$3(t^T H t)(g^T H t) - \|g\|^2 t^T \begin{pmatrix} t^T H_x t \\ t^T H_y t \end{pmatrix} = 0. \quad (5.1)$$

## 5.2. 3D Image

The 3D case is not exactly the extension of the 2D analysis because there is a different curvature for each surface direction, i.e., for each curve of the surface  $M$  including a given point  $p$  and such that the curve normal corresponds to the surface normal. A local curvature extremum is a local extremum of the maximum curvature in the maximum curvature direction (the maximum curvature is the principal curvature having the highest magnitude; the maximum curvature direction is the corresponding principal curvature direction). It is essential to remark that this definition is sound thanks to the continuity and differentiability of the principal curvature field in a regular surface (see [11] p. 156). Therefore when we calculate the derivative of the curvature  $\kappa_t$  in the direction  $\mathbf{t}$ , the curvature extrema are located where this derivative is zero in the maximum curvature direction. We note finally that a very similar definition is presented by Yuille and Leyton [32] who set the curvature extremum as the principal curvature extremum along a curvature line.

Letting  $\mathbf{t}_1$  be the maximum curvature direction, the directional derivative along  $\mathbf{t}_1$  is

$$\nabla_{\mathbf{t}_1} \kappa_{\mathbf{t}_1}(p) = \lim_{\lambda \rightarrow 0} \frac{\kappa_{\mathbf{t}_1}(p + \lambda \mathbf{t}_1) - \kappa_{\mathbf{t}_1}(p)}{\lambda} = \nabla \kappa_{\mathbf{t}_1}(p) \cdot \mathbf{t}_1 = \begin{pmatrix} (\delta \kappa_{\mathbf{t}_1} / \delta x)(p) \\ (\delta \kappa_{\mathbf{t}_1} / \delta y)(p) \\ (\delta \kappa_{\mathbf{t}_1} / \delta z)(p) \end{pmatrix} \cdot \begin{pmatrix} t_{1x} \\ t_{1y} \\ t_{1z} \end{pmatrix}.$$

From Eq.(4.13), we have

$$\kappa_{t_1}(p) = \frac{-t_1^T H t_1}{\|g\|} = \frac{-(I_{xx}t_{1x}^2 + I_{yy}t_{1y}^2 + I_{zz}t_{1z}^2 + 2I_{xy}t_{1x}t_{1y} + 2I_{xz}t_{1x}t_{1z} + 2I_{yz}t_{1y}t_{1z})}{\|g\|}.$$

As a result,

$$\nabla_{t_1} \kappa_{t_1}(p) = \frac{3(t_1^T H t_1)(t_1^T H g) - \|g\|^2 t_1^T \psi}{\|g\|^3} \tag{5.2}$$

with  $H_x, H_y$  and  $H_z$  are the partial derivatives of the Hessian matrix  $H$  and  $\psi$  as the following:

$$H_x = \frac{\partial H}{\partial x} = \begin{pmatrix} I_{xxx} & I_{xyx} & I_{xzx} \\ I_{yxx} & I_{yyx} & I_{yzx} \\ I_{zxx} & I_{zyx} & I_{zzx} \end{pmatrix}, \quad \psi = \begin{pmatrix} t_1^T H_x t_1 \\ t_1^T H_y t_1 \\ t_1^T H_z t_1 \end{pmatrix} \tag{5.3}$$

Henceforth we will call  $\nabla_{t_1} \kappa_{t_1}(p)$  the ”**extremality**” **criterion** and the necessary condition for the extrema is given as

$$3(t_1^T H t_1)(t_1^T H g) - \|g\|^2 t_1^T \psi = 0. \tag{5.4}$$

## 6. Summary of the algorithms

We summarize the algorithms implied by the formulas of the previous sections that find curvatures and ridge points on surfaces in 3D equation or (3D data).

Let  $I(x, y, z)$  be a 3D isosurface equation (3D image data). When  $I$  is 3D image we using 3D edge extractor, a collection of points are designated as ”surface points.” Since the edge extractor may use differential information, the computations may be overlapped with portions of the first step below. The following algorithm is used to compute curvatures and ridge points directly from the isosurface equation or (the 3D image data).

- (1) Compute the 19 first-, second-, and third-order partial derivatives of  $I$ , directly from the isosurface equation  $I$  (in case 3-Dimension data we using the 3D separable recursive filters given by [10, 19, 30]).
- (2) If  $I$  2D or 3D data, we will extracted the 3D edges using [1, 9, 19].

(3) For each edge point:

1- Compute the two principal curvatures and the corresponding principal curvature directions (see Section 4).

2- Compute the extremality criterion (see Section 5).

3- Using the maximum curvature and the maximum curvature direction select the edge points where the maximum curvature is locally extremum along the maximum curvature direction (in case 3D data, we use a method described in [18] very similar to the extraction of the maximum of the gradient magnitude in the gradient direction [7]).

## 7. Experimental results

We have applied the algorithm above in 2D Image and 3D Image as following

### 7.1. 2D image

Consider a contour defined as an isocontour represented by the equation

$$I(x, y) = y - x^4 + 4x^2 + 2x + 5, \quad x \in [-2, 2], \quad y \in [0.5, 12] \quad (7.1)$$

or in parametric equation representation

$$R(u) = (u, -u^4 + 4u^2 + 2u + 5), \quad u \in [-2, 2] \quad (7.2)$$

as shown in Figure 4.

From Eqs. (4.5), (4.7) the tangent vector  $\mathbf{t}$  and Hessian matrix  $\mathbf{H}$  of (7.1) are respectively

$$H = \begin{pmatrix} 8 - 12x^2 & 0 \\ 0 & 0 \end{pmatrix}, \quad t = \frac{-1}{\mu} \begin{pmatrix} 1 \\ \eta \end{pmatrix}$$

where  $\mu = (\eta^2 + 1)^{1/2}$ ,  $\eta = -4x^3 + 8x + 2$ .

From Eq.(4.6) the curvature  $\kappa_t$  of (7.1) is

$$\kappa_t = \frac{12x^2 - 8}{\mu^3}$$

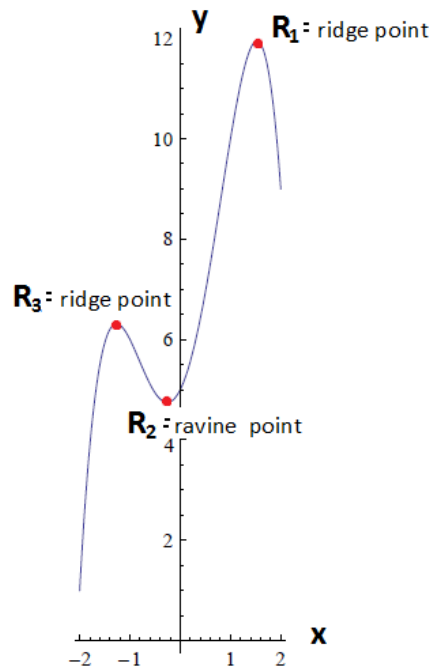


FIGURE 4. The ridge points on 2D isocontour (7.2)

From Eq.(5.1), the necessary condition for the curvature extrema is given as

$$-56x^7 + 176x^5 + 20x^4 - 160x^3 - 16x^2 + 69x + 16 = 0$$

The real roots of this equation are

$R_1=(1.527, 11.944)$ ,  $R_2=(-0.253, 4.74594)$ ,  $R_3=(-1.274, 6.30993)$ , as shown in Figure 4,  $R_1$  and  $R_3$  are ridge points and  $R_2$  is ravine point.

## 7.2. 3D image:

Consider a surface defined as an isosurface of  $I(x, y, z)$  represented by the equation

$$I(x, y, z) = z - x^4 - y^4 + x^2 + y^2, \quad x, y \in [-1.2, 1.2] \quad (7.3)$$

or in parametric equation representation

$$R(u^1, u^2) = (u^1, u^2, -(u^1)^4 - (u^2)^4 + (u^1)^2 + (u^2)^2), \quad u^1, u^2 \in [-1.2, 1.2] \quad (7.4)$$

as shown in Figure 5.

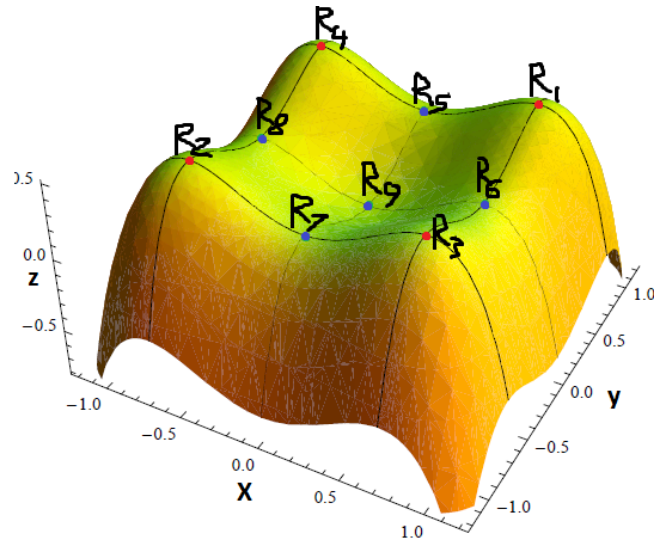


FIGURE 5. The ridge points on 3D isosurface (7.4)

From Eqs. (4.8), (4.15) the gradient vector, Hessian matrix (H) and rotation matrix (P) of (7.3) are respectively

$$g = \begin{pmatrix} 2x - 4x^3 \\ 2y - 4y^3 \\ 1 \end{pmatrix}, \quad H = \begin{pmatrix} 2 - 12x^2 & 0 & 0 \\ 0 & 2 - 12y^2 & 0 \\ 0 & 0 & 0 \end{pmatrix},$$

$$P = \begin{pmatrix} \frac{2x-4x^3}{\eta^{1/2}} & \frac{2y-4y^3}{(\eta-1)^{1/2}} & \frac{2x-4x^3}{\eta^{1/2}(\eta-1)^{1/2}} \\ \frac{2y-4y^3}{\eta^{1/2}} & \frac{-2x+4x^3}{(\eta-1)^{1/2}} & \frac{2y-4y^3}{\eta^{1/2}(\eta-1)^{1/2}} \\ \frac{1}{\eta^{1/2}} & 0 & \frac{-(\eta-1)^{1/2}}{\eta^{1/2}} \end{pmatrix} = \begin{pmatrix} n & h & f \end{pmatrix}$$

where  $\eta = (2x - 4x^3)^2 + (2y - 4y^3)^2 + 1$ .

From Eq.(4.19) the principal curvatures  $\kappa_1, \kappa_2$  of (7.3) are

$$\kappa_1 = \frac{-2\zeta + 2\sqrt{\zeta^2 - (6x^2 - 1)(6y^2 - 1)\xi}}{\xi^{3/2}}, \quad \kappa_2 = \frac{-2\zeta - 2\sqrt{\zeta^2 - (6x^2 - 1)(6y^2 - 1)\xi}}{\xi^{3/2}}$$



where  $\zeta = 8(6y^2 - 1)x^6 + (8 - 48y^2)x^4 + (1 + 24y^2 - 48y^4 + 48y^6)x^2 + (-8y^6 + 8y^4 + y^2 - 1)$ ,  $\xi = 16x^6 - 16x^4 + 4x^2 + 16y^6 - 16y^4 + 4y^2 + 1$ .

Compute the principal curvature directions  $t_1, t_2$  from Eq.(4.21) and the extrema points from Eq.(5.4) and using the Hessian matrix  $Hess\kappa_1$  of the principal curve function  $\kappa_1 = \kappa_1(x, y)$ , we have the ridge and ravine as in the following table which illustrate the Figure 5.

TABLE 1. Ridges and Ravines points on (7.3).

Extrema point	x	y	$\kappa_1$	Extrema type
$R_1$	$1/\sqrt{2}$	$1/\sqrt{2}$	-4	ridge point
$R_2$	$-1/\sqrt{2}$	$-1/\sqrt{2}$	-4	ridge point
$R_3$	$1/\sqrt{2}$	$-1/\sqrt{2}$	-4	ridge point
$R_4$	$-1/\sqrt{2}$	$1/\sqrt{2}$	-4	ridge point
$R_5$	0	$1/\sqrt{2}$	2	ravine point
$R_6$	$1/\sqrt{2}$	0	2	ravine point
$R_7$	0	$-1/\sqrt{2}$	2	ravine point
$R_8$	$-1/\sqrt{2}$	0	2	ravine point
$R_9$	0	0	2	ravine point

## 8. Conclusion

We have presented a new approach to extract principal curvatures, principal directions, ridges and ravines characteristics of isosurface in 2D and 3D images from the gradient, Hessian matrix and its derivatives (i.e. the first, second, third and fourth partial derivatives) of isosurface.

## REFERENCES

[1] N. H. Abdel-All, M. A. Soliman, R. A. Hussien and W. M. El-Nini, Geometric Image Edge Detection Techniques, *Int. J. Math. Comput. Applics. Res.*, 3 (2013) 1-14.

- [2] N. H. Abdel-All and A. A. Al-moneef, Ridges and Singularities on Hypersurfaces. *Jour. Inst. maths.& Comp. Sciences (Maths. Ser.)*, 21 (2008) 109-116.
- [3] N. H. Abdel-All and A. A. Al-moneef, Generalized Ridgea and Raines on an Equiform Motion. *Studies in Mathematical sciences*, 4 (2012) 76-85.
- [4] N. H. Abdel-All and A. A. Al-moneef, Local Study of Sigularities on an Equiform Motion. *Studies in Mathematical sciences*, 5 (2012) 26-36.
- [5] F. L. Bookstein and C. B. Cutting, A proposal for the apprehension of curving craniofacial form in three dimensions. In *K. Vig and B. A., editors, Craniofacial Morphogenesis and Dysmorphogenesis*, (1988) 127-140.
- [6] M. Brady, J. Ponce, A. Yuille, and H. Asada, Describing surfsces, in *Proceedings of the Second International Symposium on Robotics Research*, (1985) 5-16.
- [7] J. Canny, A computational approach to edge detection, *IEEE Trans. Pattern Anal. Mach. Intell.*, 8 (1986) 679-689.
- [8] J. Declerck, G. Subsol, J.-P. Thirion, and N. Ayache. Automatic retrieval of anatomical structures in 3d medical images. *INRIA, Le Chesnay, France*, 1995.
- [9] R. Deriche, Using Canny's criteria to derive a recursively implemented optimal edge detector,, *Int. J. Comput. Vision*, (1987) 167-187.
- [10] R. Deriche, Fast algorithms for low level vision, *IEEE Trans. Pattern Anal. Mach. Intell.*, 12 (1989) 78-87.
- [11] M. P. Do-Carmo, Differential Geometry of Curves and Surfaces, *Prentice-Hall, Englewood Cliffs, NJ*, 1976.
- [12] D. Eberly. Ridges in Image and Data Analysis. *Kluwer*, 1996.
- [13] G. G. Gordon. Face recognition from depth maps and surface curvature. In *Geometric Methods in Computer Vision, Proc. SPIE 1570*, (1991) 234-247.
- [14] M. Hosaka. Modeling of Curves and Surfaces in CAD/CAM. *Springer, Berlin*, 1992.
- [15] M. J. J. Koenderink, Solid Shape, *MIT Press, Boston*, 1990.
- [16] T. Maekawa and N. M. Patrikalakis. Interrogation of differential geometry properties for design and manufacture. *The Visual Computer*, 10 (1994) 216-237.
- [17] G. Medioni and R. Nevatia. Description of 3-d surfaces using curvature properties. In *Proc. DARPA Image Understanding Workshop*, (1984) 291-299.
- [18] O. Monga and N. Ayache and P. Sander, From voxel to curvature, in *IEEE Conference on Vision and Pattern Recognition, Hawaii*, 1991.
- [19] O. Monga R. Deriche and G. Malandaing, Recursive filtering and edge closing: Two primary tools for 3D edge detection, *Image Vision comput.*, 9 (1991) 1-19.

- [20] O. Monga, R. Deriche and J. M. Rocchisani, 3D edge detection using recursive filtering: Application to scanner images, *Copmut. Vision Graphic Image Process.*, 53 (1991) 76-87.
- [21] O. Monga, N. Armande, and P. Montesinos. Thin nets and crest lines: application to satellite data and medical images. *Rapport de Recherche 2480, INRIA, Le Chesnay, France*, 1995.
- [22] O. Monga and S. Benayoun. Using partial derivatives of 3d images to extract typical surface features. *Computer Vision and Image Understanding*, 61 (1995) 171-189.
- [23] T. Mullaria, U. Kottaa, Z. Bartosiewiczb and E. Pawluszewicz, The concepts of Lie derivative for discrete-time systems, *Proceedings of the Estonian Academy of Sciences*, 61 (2012) 253-265.
- [24] B. O'Neill, Elementary Differential Geometry. *Academic Press, San Diego, CA, 2nd edition*, 1997.
- [25] J. Ponce and M. Brady, Toward a surface primal sketch, in *Proceedings, IJCAI*, 1985.
- [26] I. R. Porteous. Geometric Differentiation for the Intelligence of Curves and Surfaces. *Cambridge University Press, Cambridge*, 1994.
- [27] P. T. Sander and S. W. Zucker, Tracing surfaces for surfacing traces, in *Proceedings of the First International Conference on Computer Vision, London*, (1987) 241-249.
- [28] P. T. Sander and S. W. Zucker, Inferring surface trace and differential structure from 3D images, *IEEE Trans. Pattern Anal. Mach. Intell.*, 12 (1990).
- [29] J. P. Thirion and A. Gourdon. The marching lines algorithm: new results and proofs. *Rapport de Recherche 1881, INRIA, Le Chesnay, France*, 1993.
- [30] T. Vieville and O. Faugeras, Robust and fast computation of high order spatial derivatives in images sequences, *INRIA research report*, 1992.
- [31] A. Yuille. Zero crossings on lines of curvature. *CVGIP*, 45 (1989) 68-87.
- [32] A. Yuille and M. Leyton, 3D symmetry-curvature duality theorems, *Comput. Vision Graphics Images Process.*, 52 (1990) 124-140.
- [33] S. W. Zucker and R. M. Hummel, Athree-dimensional edge operator, *IEEE Trans. Pattern Anal. Mach. Intell.*, 3 (1981) 324-331.